

## Accepted Article

**Title:** GOx@ZIF-8(NiPd) nanoflower: an artificial enzyme system for tandem catalysis

**Authors:** Qingqing Wang, Xueping Zhang, Liang Huang, Zhiquan Zhang, and Shaojun Dong

This manuscript has been accepted after peer review and appears as an Accepted Article online prior to editing, proofing, and formal publication of the final Version of Record (VoR). This work is currently citable by using the Digital Object Identifier (DOI) given below. The VoR will be published online in Early View as soon as possible and may be different to this Accepted Article as a result of editing. Readers should obtain the VoR from the journal website shown below when it is published to ensure accuracy of information. The authors are responsible for the content of this Accepted Article.

**To be cited as:** *Angew. Chem. Int. Ed.* 10.1002/anie.201710418  
*Angew. Chem.* 10.1002/ange.201710418

**Link to VoR:** <http://dx.doi.org/10.1002/anie.201710418>  
<http://dx.doi.org/10.1002/ange.201710418>

# GOx@ZIF-8(NiPd) nanoflower: an artificial enzyme system for tandem catalysis

Qingqing Wang,<sup>[a, b]</sup> Xueping Zhang,<sup>[b]</sup> Liang Huang,<sup>[b]</sup> Zhiquan Zhang,<sup>\*[a]</sup> and Shaojun Dong<sup>\*[b]</sup>

**Abstract:** This work reports a facile approach to fabricate an artificial enzyme system for tandem catalysis. NiPd hollow nanoparticles and glucose oxidase (GOx) were simultaneously immobilized on the zeolitic imidazolate framework 8 (ZIF-8) via a co-precipitation method. The as-prepared GOx@ZIF-8(NiPd) nanoflower not only exhibited the peroxidase-like activity of NiPd hollow nanoparticles but also maintained the enzymatic activity of GOx. A colorimetric sensor for rapid detection of glucose was fabricated through the GOx@ZIF-8(NiPd) based multi-enzyme system and the cascade reaction for the visual detection of glucose was successfully combined into one step. Moreover, the GOx@ZIF-8(NiPd) modified electrode showed good bioactivity of GOx and high electrocatalytic activity for the oxygen reduction reaction (ORR), which could also be used for electrochemical detection of glucose. The proposed strategy for the fabrication of artificial multi-enzyme system builds a potential bridge of cooperation between nanozyme and natural enzyme, combining together their properties and functionalities, as well making efforts to multi-catalysis and tandem reactions.

Metal-organic frameworks (MOFs),<sup>[1]</sup> which are self-assembled from organic ligand and metal ions, have attracted immense attention owing to their large and accessible specific surface areas, uniform and tunable pore sizes.<sup>[2]</sup> Recently, a series of mesoporous metalloporphyrin Fe-MOFs have been demonstrated as an effective peroxidase mimic to catalyze the oxidation reaction.<sup>[3]</sup> Various MOFs or modified MOFs have been reported as enzyme mimetics with biological functions,<sup>[4]</sup> expanding their applications in biotechnology fields such as bioanalysis, biocatalysis, and biomedical engineering.<sup>[5]</sup> In particular, coating enzyme with ZIF-8 could protect the biomacromolecules from biological, thermal and chemical degradation with maintenance of bioactivity,<sup>[6]</sup> and Cyt c/ZIF-8 composite was found exhibiting a 10-fold increase in peroxidase activity compared to free cytochrome c (Cyt c) in solution.<sup>[7]</sup> Inspired by the merits of ZIF-8, more and more attentions have been paid to biomimetic mineralization of ZIF-8.<sup>[8]</sup>

In our work, ZIF-8 was chosen as a support for enzyme immobilization to establish a mimic multi-enzyme system. NiPd

hollow nanoparticles, which exhibiting outstanding peroxidase-like catalytic activity,<sup>[9]</sup> were successfully immobilized both inside of the ZIF-8 crystal lattices and on the outer surfaces. The obtained ZIF-8(NiPd) also possessed excellent property of peroxidase mimic. With glucose oxidase (GOx) and NiPd hollow nanoparticles being immobilized simultaneously on ZIF-8, an artificial enzyme system GOx@ZIF-8(NiPd) nanoflower was prepared for tandem catalysis. The cascade reaction for the visual detection of glucose was successfully combined into one step. In addition, due to the competition reactions of electrocatalytic oxygen reduction and glucose oxidation, the GOx@ZIF-8(NiPd) modified glassy carbon electrode (GCE) exhibits quiet different electrochemical performance toward H<sub>2</sub>O<sub>2</sub> and glucose. As a result, a novel electrochemical sensor for glucose detection could also be fabricated based on the obtained nanoflower. More importantly, our strategy was applicable to other nanozymes<sup>[10]</sup> and proteins such as Cyt c and horseradish peroxidase (HRP). Various kinds of multi-enzyme system would be fabricated, making further effort to mimic complex natural enzyme system.

By using PVP as the nanoparticle stabilizer, NiPd hollow nanoparticles could be located both inside and on the outer surface of ZIF-8 crystal when PVP-stabilized nanoparticles were added into the ZIF-8 synthesis solution at short time (less than 2 min). Via a co-precipitation procedure in aqueous solution, GOx and NiPd hollow nanoparticles could be simultaneously immobilized in ZIF-8. After being encapsulated into ZIF-8, GOx reserved the enzymatic activity because the assembling process is very gentle and environmental friendly. The strategy could not only prevent the enzymes from leaching but also build a potential bridge of cooperation between nanozyme and natural enzyme, thus opening a new avenue for combining together their properties and functionalities.

The obtained ZIF-8 based nanocomposites (**Figure S1**) showed different colors with each other because different guests were encapsulated in the ZIF-8 hosts. The morphology of the samples was further characterized by TEM and SEM. As displayed in **Figure 1c** and **1d**, the hollow nanoparticles are distributed on the ZIF-8, and the average diameter of NiPd hollow nanoparticles is about 40 nm (**Figure S2a**). ZIF-8(NiPd) maintained the morphology of ZIF-8, which has a regular smooth fusiform structure as shown in **Figure S2b**. Some cruciate flower-like structure (**Figure 1c**) was also observed in ZIF-8(NiPd), which can be ascribed as the two ZIF-8 nanoparticles assembled simultaneously during the growth of nanocrystals. However, compared with ZIF-8, the size of GOx@ZIF-8 turned smaller and the morphology changed obviously (**Figure 1e** and **1f**). The novel nanoflower structure of GOx@ZIF-8 would be facilitated by the GOx affinity towards the imidazole-containing building block arising from intermolecular hydrogen bonding and hydrophobic interactions.<sup>[11]</sup> The GOx-ZIF-8 interaction was

[a] Q. Wang, Prof. Z. Zhang  
College of Chemistry, Jilin University, Changchun, 130012, P. R. China  
E-mail: zzq@jlu.edu.cn.

[b] Q. Wang, X. Zhang, L. Huang, Prof. S. Dong  
State Key Laboratory of Electroanalytical Chemistry, Changchun Institute of Applied Chemistry, Changchun, 130022, P. R. China  
E-mail: dongsj@ciac.ac.cn.

Supporting information for this article is given via a link at the end of the document.

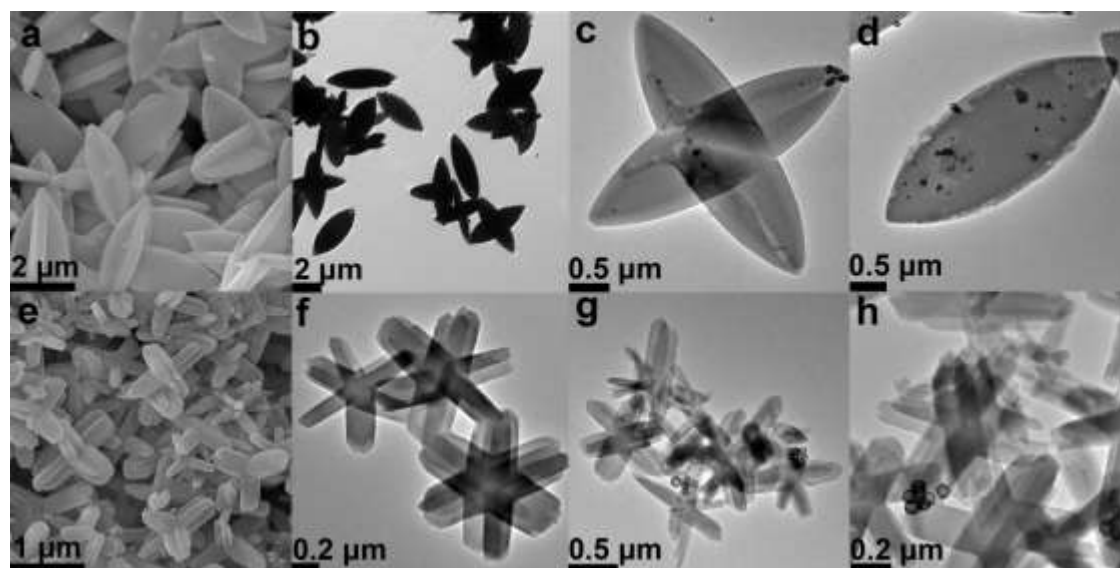


**Figure 1.** (a) SEM images of ZIF-8(NiPd). (b), (c) and (d) TEM images of ZIF-8(NiPd). (e) SEM images of GOx@ZIF-8. (f) TEM images of GOx@ZIF-8. (g) and (h) TEM images of GOx@ZIF-8(NiPd).

probably due to the coordination between the Zn cations and the carbonyl group of the proteins.<sup>[6b, 12]</sup> With the similar one-pot strategy, NiPd hollow nanoparticles and GOx were successfully encapsulated in ZIF-8, forming a mimic multi-enzyme system GOx@ZIF-8(NiPd) (**Figure 1g** and **1h**). Interestingly, the XRD patterns of the nanocomposites (GOx@ZIF-8(NiPd), GOx@ZIF-8 and ZIF-8(NiPd)) were almost identical to the measured patterns of ZIF-8, indicating that the encapsulation of NiPd or GOx had negligible effects on the phase of ZIF-8 hosts (**Figure 2a**). The FTIR spectra (**Figure 2b**) showed stretches characteristic of GOx at  $\sim 1640\text{--}1660\text{ cm}^{-1}$ , corresponding to amide I, mainly attributed to C=O stretching mode. This result suggested the presence of GOx in the GOx@ZIF-8(NiPd) and GOx@ZIF-8 composites.

To investigate the mimic enzyme catalytic activity of ZIF-8(NiPd), typical peroxidase substrate OPD was chosen as the chromogenic substrate. As shown in **Figure S4**, ZIF-8(NiPd) could catalyze the oxidation of OPD to produce a typical yellow oxidized product 2,3-diaminophenazinc (DAP) in the presence of H<sub>2</sub>O<sub>2</sub> (curve 3), indicating the peroxidase-like activity of ZIF-8(NiPd). Additionally, the absorbance changes of OPD were investigated at different pH (pH 3.0–10.0) and temperature (20–

90 °C) ranges. Because of the negligible background signal, pH = 4.0 and 50 °C were adopted for the subsequent activity analysis of ZIF-8(NiPd) (**Figure S5**). The apparent steady-state kinetic parameters for this reaction were determined by changing the concentration of OPD and H<sub>2</sub>O<sub>2</sub> in the system, respectively (**Figure S7**). The oxidation reaction catalyzed by ZIF-8(NiPd) follows the typical Michaelis–Menten behavior toward both substrates, OPD and H<sub>2</sub>O<sub>2</sub> (**Figure S7a** and **S7c**). The value  $\epsilon = 17\,000\text{ M}^{-1}\text{ cm}^{-1}$  (at 417 nm) for DAP was used here to obtain the corresponding concentration term from the absorbance data. By using Lineweaver–Burk plot (**Figure S7b** and **S7d**),  $K_m$  and  $V_m$  were obtained as given in **Table S1**. Compared with horseradish peroxidase (HRP) and other ZIF-8-based catalysts shown in **Table S1**, the apparent  $K_m$  value of ZIF-8(NiPd) with OPD or H<sub>2</sub>O<sub>2</sub> as the substrate is lower, indicating the higher catalytic activity of ZIF-8(NiPd).

In the following experiments, potential enzymatic performance of GOx@ZIF-8(NiPd) was determined in detail. As shown in **Figure 3a**, the absorbance enhanced with the increase of the reaction time, indicating the peroxidase-like activity of GOx@ZIF-8(NiPd). And with the same content of NiPd, the catalytic activity of GOx@ZIF-8(NiPd) was similar to that of ZIF-8(NiPd) and NiPd hollow nanoparticles, suggesting that the introduce of GOx and ZIF-8 had negligible effect on the catalytic activity of the NiPd hollow nanoparticles. Then, the enzymatic activity of the GOx encapsulated in GOx@ZIF-8(NiPd) was detected by a gluconic acid-specific colorimetric assay<sup>[13]</sup> as GOx could catalyze the oxidation of glucose yielding gluconic acid and H<sub>2</sub>O<sub>2</sub>. Upon the addition of hydroxamine and Fe<sup>3+</sup>, the color of the solution turned red with a characteristic absorbance peak at 505 nm (**Figure 3b**), which suggested that gluconic acid was indeed produced in this GOx@ZIF-8(NiPd)-catalyzed reaction. The solutions containing glucose or GOx@ZIF-8(NiPd) alone could not introduce any color change. In particular, GOx@ZIF-8(NiPd) exhibited much higher catalytic activity than

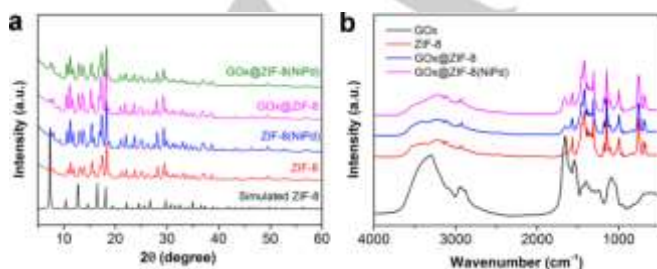


**Figure 2.** (a) XRD patterns of GOx@ZIF-8(NiPd), GOx@ZIF-8, ZIF-8(NiPd), ZIF-8 and simulated ZIF-8. (b) FTIR spectra of GOx, ZIF-8, GOx@ZIF-8 and GOx@ZIF-8(NiPd).

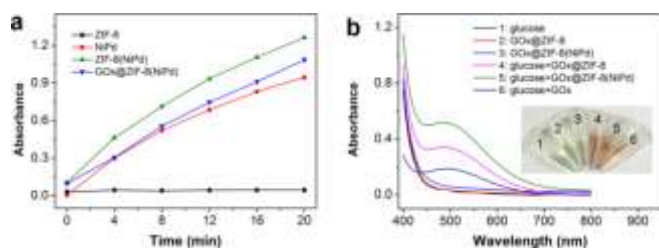


**Figure 3.** (a) Time-dependent absorbance changes at 417 nm of OPD using different catalysts. (b) UV-Vis absorbance spectra and visual color changes for different samples obtained by a gluconic acid-specific assay.

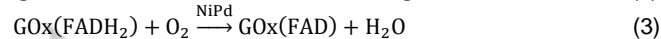
GOx@ZIF-8 although both of them can catalyze the oxidation of glucose. The higher catalytic activity can be ascribed to the hollow nanoparticle structure of NiPd in GOx@ZIF-8(NiPd), which could help capturing more GOx molecules into ZIF-8, improving the catalytic activity of the composite. As a result, the as-prepared GOx@ZIF-8(NiPd) nanoflower not only exhibited the peroxidase-like activity of NiPd hollow nanoparticles but also reserved the enzymatic activity of GOx.

A multi-enzyme system could be fabricated based on GOx@ZIF-8(NiPd) nanoflower, and the feasibility of cascade reaction was verified. That is, GOx@ZIF-8(NiPd) first catalyzed the glucose oxidation to yield gluconic acid and  $\text{H}_2\text{O}_2$  by means of molecular oxygen, and then catalyzed the oxidation of OPD by produced  $\text{H}_2\text{O}_2$  resulting in the formation of a colored product of DAP [eq. 1]:

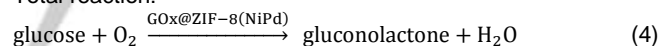


As shown in **Figure S8**, the cascade reaction for the visual detection of glucose could be combined into one step, and the optimized conditions of pH 4.0 and 50 °C were adopted for subsequent one-pot detection of glucose. With the increase of the glucose concentration, the absorbance of the solution increased gradually and its corresponding solution color changed from very light yellow to deep yellow (**Figure S9a**). There is a good linear relationship between the absorbance of DAP and glucose concentrations in the range of 0.01-0.3 mM with a limit of detection (LOD) of 9.2  $\mu\text{M}$ , which was comparative to other colorimetric methods as shown in **Table S2**. Moreover, the specificity of the colorimetric sensor was tested using other saccharides such as fructose, maltose, lactose, and sucrose. The color difference can be distinguished by the naked eye as shown in **Figure S9b**, suggesting a good selectivity of the developed glucose biosensor.

We also investigated the electrocatalytic activity of GOx@ZIF-8(NiPd) in detail. As shown in **Figure 4a**, the cathodic peak current at about -0.45 V increased when the  $\text{H}_2\text{O}_2$  concentration rose from 0 to 10 mM, indicating the electrocatalytic activity of GOx@ZIF-8(NiPd) towards the reduction of  $\text{H}_2\text{O}_2$ . To be surprised, the cathodic peak current decreased significantly with the increase of glucose concentration (**Figure 4b**). The mechanism of the process was quite different from the reported glucose electrochemical sensor based on GOx and peroxidase mimics. The reduction peaks of GOx@ZIF-8(NiPd)/GCE in **Figure 4b** would be generated mainly from ORR. With the addition of glucose, GOx@ZIF-8(NiPd)/GCE could catalyze the oxidation of glucose and decrease the concentration of dissolved oxygen in the solution, resulting in an obvious drop of the cathodic peak current of ORR. Therefore, the signal of glucose could be distinguished easily with that of  $\text{H}_2\text{O}_2$  by the opposite response current as shown in **Figure 4c**. For comparison, the electrochemical performance of ZIF-8(NiPd)/GCE towards  $\text{H}_2\text{O}_2$  and glucose was also investigated respectively. As displayed in **Figure S10a** and **S10b**, ZIF-8(NiPd)/GCE could also electro-catalyze the reduction of  $\text{H}_2\text{O}_2$ , but no obvious changes were found at the cathodic peak current in the presence of glucose because glucose oxidation could not happen without GOx. **Figure S10c** and **S10d** further demonstrated that GOx@ZIF-8(NiPd)/GCE and ZIF-8(NiPd)/GCE both possessed high electrocatalytic activity towards ORR, which originated from the encapsulation of NiPd. A direct 4-electron reduction pathway for ORR possibly occurred at the modified electrode. The mechanism of the process could be expressed as following [eqs 2 and 3]:



Total reaction:



Based on the competitive reactions of oxygen reduction and glucose oxidation, electrochemical glucose biosensors could be fabricated.<sup>[14]</sup> As shown in **Figure 4c**, GOx@ZIF-8(NiPd)/GCE could be used for glucose sensing. The response current increased to reach a steady-state with addition of  $\text{H}_2\text{O}_2$  and reduced steeply with addition of glucose under constant potential of -0.45 V. The relative standard deviation (RSD) for 16 successive determinations was 0.8% for glucose detection, suggesting good stability and reproducibility of the glucose biosensor. A well-defined linear relationship between

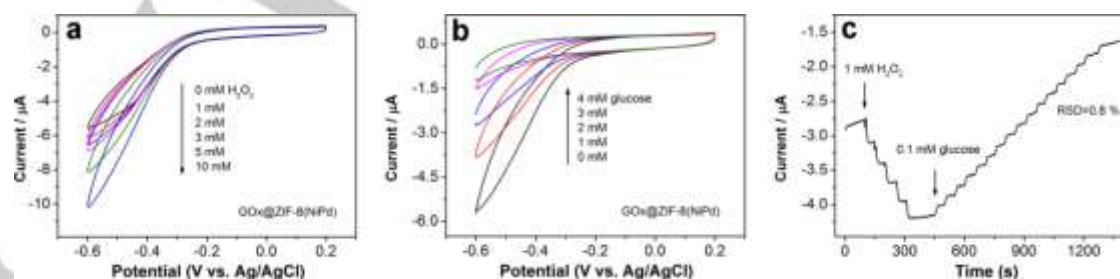


**Figure 4.** (a) CVs at GOx@ZIF-8(NiPd)/GCE in 10 mM pH 7.0 PBS containing 0, 1, 2, 3, 5, 10 mM  $\text{H}_2\text{O}_2$ . Scan rate is 50  $\text{mV s}^{-1}$ . (b) CVs at GOx@ZIF-8(NiPd)/GCE in 10 mM pH 7.0 PBS containing 0, 1, 2, 3, 4 mM glucose. (c) Amperometric time curves at GOx@ZIF-8(NiPd)/GCE in 10 mM pH 7.0 PBS upon successive injection of 1 mM  $\text{H}_2\text{O}_2$  or 0.1 mM glucose for each step at -0.45 V.

the current and glucose concentration can be observed from 0.1 to 1.7 mM (**Figure S11**). The new electrochemical glucose biosensor exhibits much wider range of glucose detection than that of mentioned colorimetric sensor, expanding the applications of bioanalysis.

In summary, we have fabricated a colorimetric and electrochemical glucose sensor based on the multi-enzyme system GOx@ZIF-8(NiPd). GOx@ZIF-8(NiPd) not only exhibited the peroxidase-like activity but also could catalyze the oxidation of glucose. Besides, GOx@ZIF-8(NiPd)/GCE possessed high electrocatalytic activity for ORR and showed good electrochemical performance toward glucose. We also believe that the obtained ZIF-8(NiPd) has the ability of the molecule-size-selective catalysis in the hydrogenation. In a word, we reported a simple, facile and green method for the direct synthesis of enzyme-embedded MOFs with multi-catalysis properties, and the obtained nanocomposites exhibited special nanoflower structure. Given the variety of nanozyme and proteins, this new method opens an avenue for combining together their properties and functionalities, displaying important features enabling applications in biosensors, biofuel cells, analytical devices and industrial catalysis.

## Acknowledgements

This work was supported by the National Natural Science Foundation of China (Nos. 21375123 and 21675151) and the Ministry of Science and Technology of China (Nos. 2013YQ170585 and 2016YFA0203201).

**Keywords:** GOx@ZIF-8(NiPd) nanoflower • artificial enzyme system • tandem catalysis • oxygen reduction reaction • glucose detection

- [1] aH. Furukawa, K. E. Cordova, M. O'Keeffe, O. M. Yaghi, *Science* **2013**, *341*; bO. M. Yaghi, M. O'Keeffe, N. W. Ockwig, H. K. Chae, M. Eddaoudi, J. Kim, *Nature* **2003**, *423*, 705-714; cH.-C. Zhou, J. R. Long, O. M. Yaghi, *Chem. Rev.* **2012**, *112*, 673-674.
- [2] aR. E. Morris, P. S. Wheatley, *Angew. Chem. Int. Ed.* **2008**, *47*, 4966-4981; bM. Maes, L. Alaerts, F. Vermoortele, R. Ameloot, S. Couck, V. Finsy, J. F. M. Denayer, D. E. De Vos, *J. Am. Chem. Soc.* **2010**, *132*, 2284-2292; cJ.-R. Li, J. Scully, H.-C. Zhou, *Chem. Rev.* **2012**, *112*, 869-932; dQ. Yang, Q. Xu, S.-H. Yu, H.-L. Jiang, *Angew. Chem. Int. Ed.* **2016**, *55*, 3685-3689; eJ.-D. Xiao, Q. Shang, Y. Xiong, Q. Zhang, Y. Luo, S.-H. Yu, H.-L. Jiang, *Angew. Chem. Int. Ed.* **2016**, *55*, 9389-9393.
- [3] K. Wang, D. Feng, T.-F. Liu, J. Su, S. Yuan, Y.-P. Chen, M. Bosch, X. Zou, H.-C. Zhou, *J. Am. Chem. Soc.* **2014**, *136*, 13983-13986.
- [4] aD. Feng, Z.-Y. Gu, J.-R. Li, H.-L. Jiang, Z. Wei, H.-C. Zhou, *Angewandte Chemie* **2012**, *124*, 10453-10456; bX.-S. Wang, M. Chrzanowski, D. Yuan, B. S. Sweeting, S. Ma, *Chem. Mater.* **2014**, *26*, 1639-1644; cR. W. Larsen, L. Wojtas, J. Perman, R. L. Musselman, M. J. Zaworotko, C. M. Vetromile, *J. Am. Chem. Soc.* **2011**, *133*, 10356-10359.
- [5] aP. Horcajada, R. Gref, T. Baati, P. K. Allan, G. Maurin, P. Couvreur, G. Férey, R. E. Morris, C. Serre, *Chem. Rev.* **2012**, *112*, 1232-1268; bJ. Zhuang, C.-H. Kuo, L.-Y. Chou, D.-Y. Liu, E. Weerapana, C.-K. Tsung, *ACS Nano* **2014**, *8*, 2812-2819; cH. Zheng, Y. Zhang, L. Liu, W. Wan, P. Guo, A. M. Nyström, X. Zou, *J. Am. Chem. Soc.* **2016**, *138*, 962-968; dJ. S. Kahn, L. Freage, N. Enkin, M. A. A. Garcia, I. Willner, *Adv. Mater.* **2017**, *29*, 1602782-n/a; eY. Hu, H. Cheng, X. Zhao, J. Wu, F. Muhammad, S. Lin, J. He, L. Zhou, C. Zhang, Y. Deng, P. Wang, Z. Zhou, S. Nie, H. Wei, *ACS Nano* **2017**, *11*, 5558-5566.
- [6] aX. Wu, C. Yang, J. Ge, Z. Liu, *Nanoscale* **2015**, *7*, 18883-18886; bK. Liang, R. Ricco, C. M. Doherty, M. J. Styles, S. Bell, N. Kirby, S. Mudie, D. Haylock, A. J. Hill, C. J. Doonan, P. Falcaro, *Nat. Commun.* **2015**, *6*, 7240; cF.-S. Liao, W.-S. Lo, Y.-S. Hsu, C.-C. Wu, S.-C. Wang, F.-K. Shieh, J. V. Morabito, L.-Y. Chou, K. C. W. Wu, C.-K. Tsung, *J. Am. Chem. Soc.* **2017**, *139*, 6530-6533; dX. Lian, Y. Fang, E. Joseph, Q. Wang, J. Li, S. Banerjee, C. Lollar, X. Wang, H.-C. Zhou, *Chem. Soc. Rev.* **2017**, *46*, 3386-3401.
- [7] F. Lyu, Y. Zhang, R. N. Zare, J. Ge, Z. Liu, *Nano Lett.* **2014**, *14*, 5761-5765.
- [8] aC. Hou, Y. Wang, Q. Ding, L. Jiang, M. Li, W. Zhu, D. Pan, H. Zhu, M. Liu, *Nanoscale* **2015**, *7*, 18770-18779; bH. Cheng, L. Zhang, J. He, W. Guo, Z. Zhou, X. Zhang, S. Nie, H. Wei, *Anal. Chem.* **2016**, *88*, 5489-5497; cY. Yin, C. Gao, Q. Xiao, G. Lin, Z. Lin, Z. Cai, H. Yang, *ACS Appl. Mat. Interfaces* **2016**, *8*, 29052-29061.
- [9] Q. Wang, L. Zhang, C. Shang, Z. Zhang, S. Dong, *Chem. Commun.* **2016**, *52*, 5410-5413.
- [10] aL. Z. Gao, J. Zhuang, L. Nie, J. B. Zhang, Y. Zhang, N. Gu, T. H. Wang, J. Feng, D. L. Yang, S. Perrett, X. Yan, *Nat. Nanotechnol.* **2007**, *2*, 577-583; bH. Wei, E. Wang, *Chem. Soc. Rev.* **2013**, *42*, 6060-6093; cH. Wei, E. Wang, *Anal. Chem.* **2008**, *80*, 2250-2254; dQ. Wang, X. Zhang, L. Huang, Z. Zhang, S. Dong, *ACS Appl. Mat. Interfaces* **2017**, *9*, 7465-7471.
- [11] aA. Lukton, *Nature* **1961**, *192*, 422-424; bE. Cauët, M. Rooman, R. Wintjens, J. Liévin, C. Biot, *J. Chem. Theory Comput.* **2005**, *1*, 472-483.
- [12] Y. Feng, A. Schmidt, R. A. Weiss, *Macromolecules* **1996**, *29*, 3909-3917.
- [13] W. Luo, C. Zhu, S. Su, D. Li, Y. He, Q. Huang, C. Fan, *ACS Nano* **2010**, *4*, 7451-7458.
- [14] Y. Tang, B. L. Allen, D. R. Kauffman, A. Star, *J. Am. Chem. Soc.* **2009**, *131*, 13200-13201.

## Entry for the Table of Contents

## COMMUNICATION

**Tandem catalysis:** NiPd hollow nanoparticles and glucose oxidase (GOx) were simultaneously immobilized on ZIF-8 via a co-precipitation method. The proposed strategy for the fabrication of artificial multi-enzyme system builds a potential bridge of cooperation between nanozyme and natural enzyme.



Q. Wang, X. Zhang, L. Huang, Prof. Z. Zhang\*, Prof. S. Dong\*

Page No. – Page No.

**GOx@ZIF-8(NiPd) nanoflower: an artificial enzyme system for tandem catalysis**